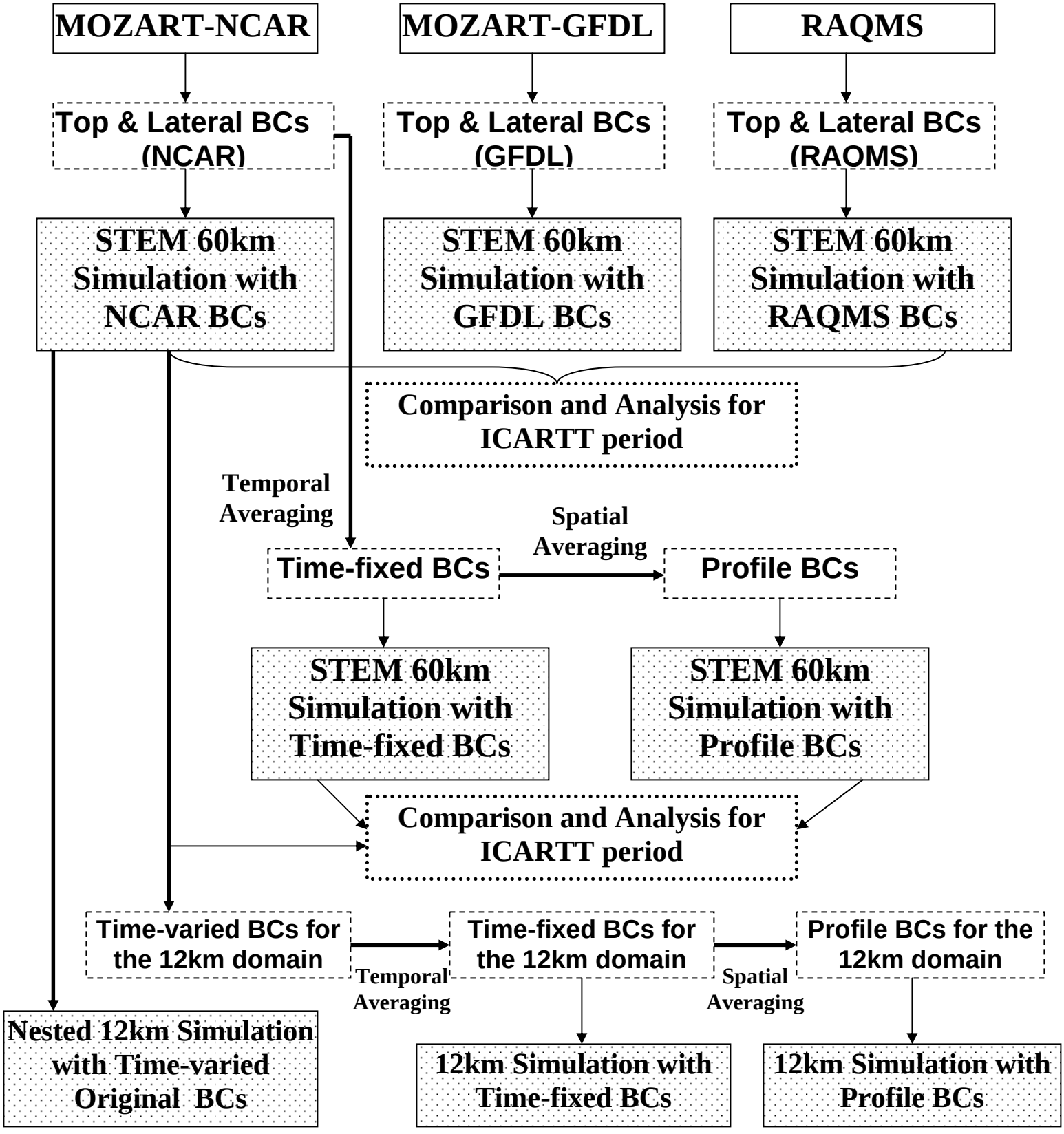

Figure 1. Comparison and Analysis Framework

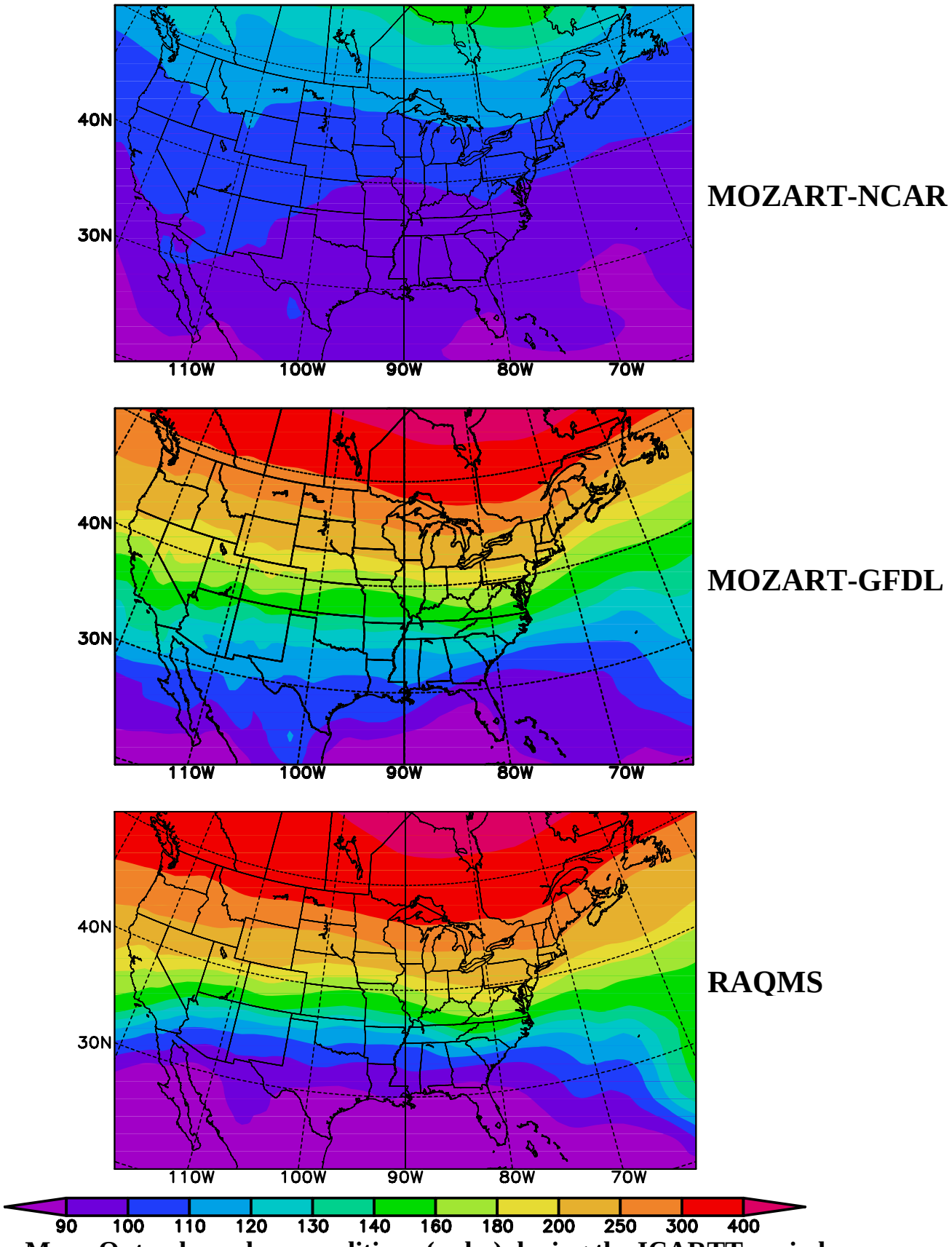

Figure 2. Period-mean O_3 top boundary conditions from 3 global models.

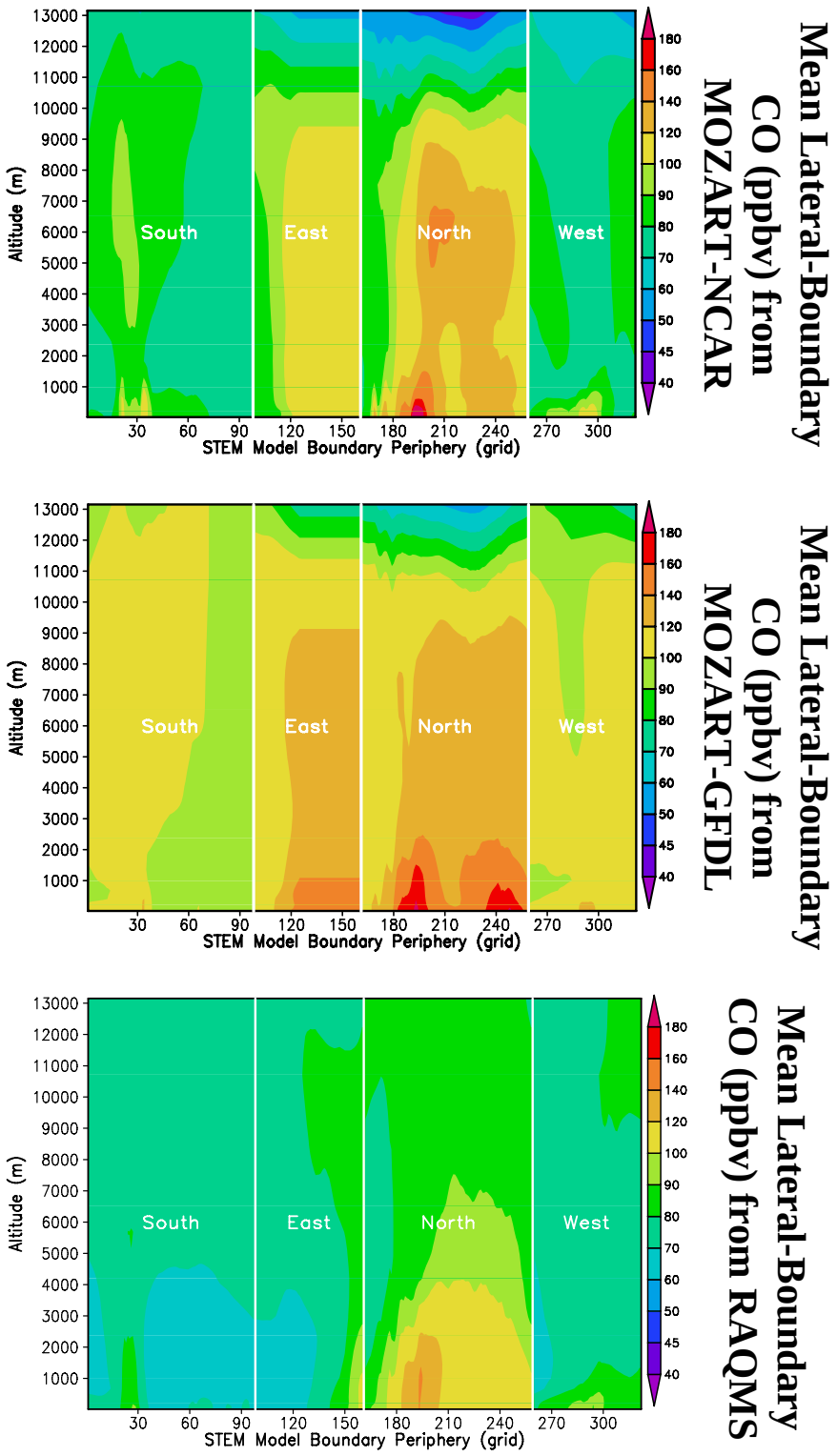

Figure 3. Period-mean CO lateral boundary conditions from 3 global models, along the STEM's boundary periphery in grid (60km) starting from the southwest corner of the STEM 60km domain shown in Figure 1.

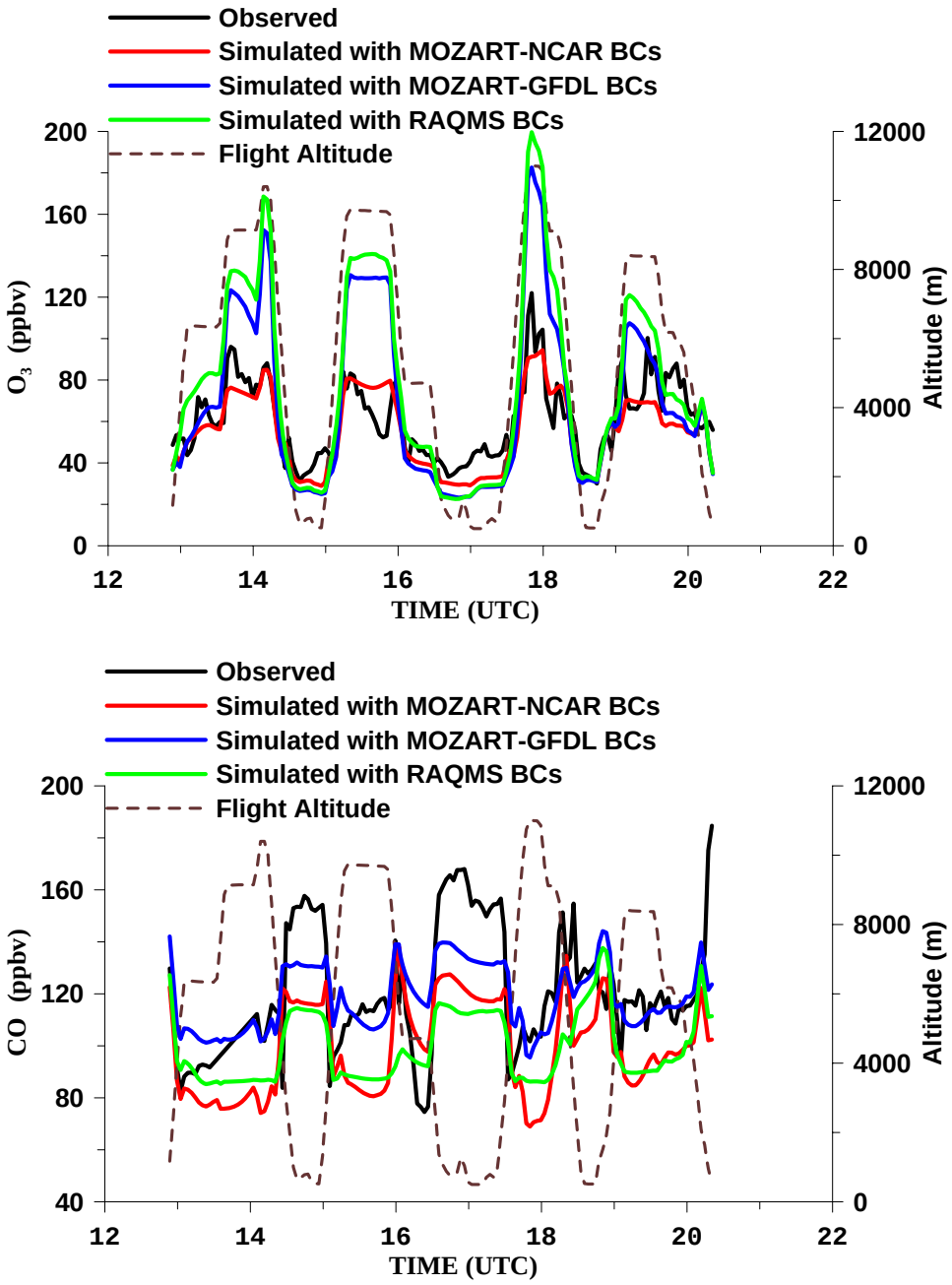

Figure 4. Observed and Simulated O_3 and CO concentrations for the DC-8 flight 8 on 07/15/2004

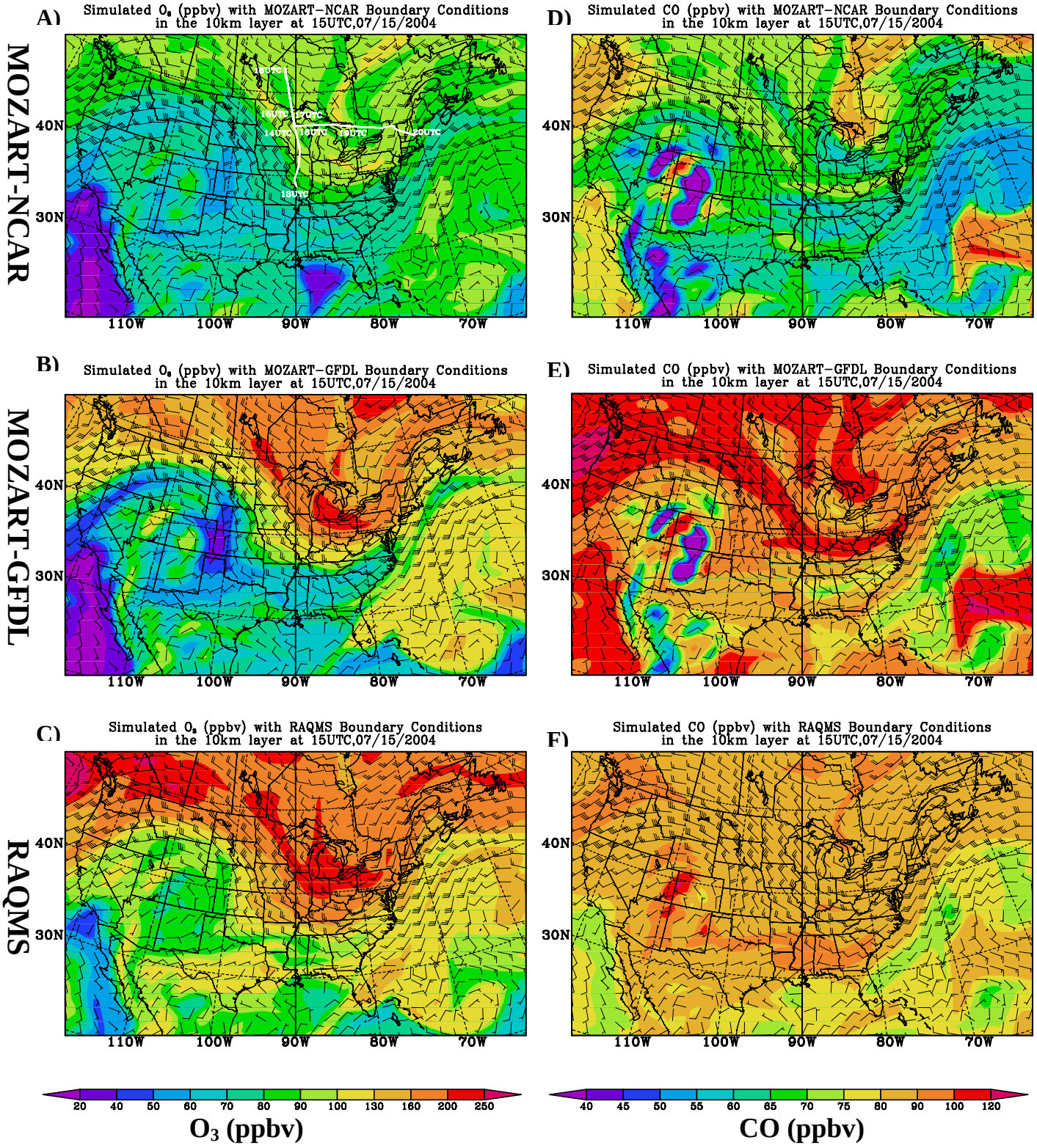

Figure 5. STEM 60km simulated O_3 and CO concentrations in the 10km layer with boundary conditions from the three global models for DC-8 flight 8 on July 15 (plot A shows the flight path).

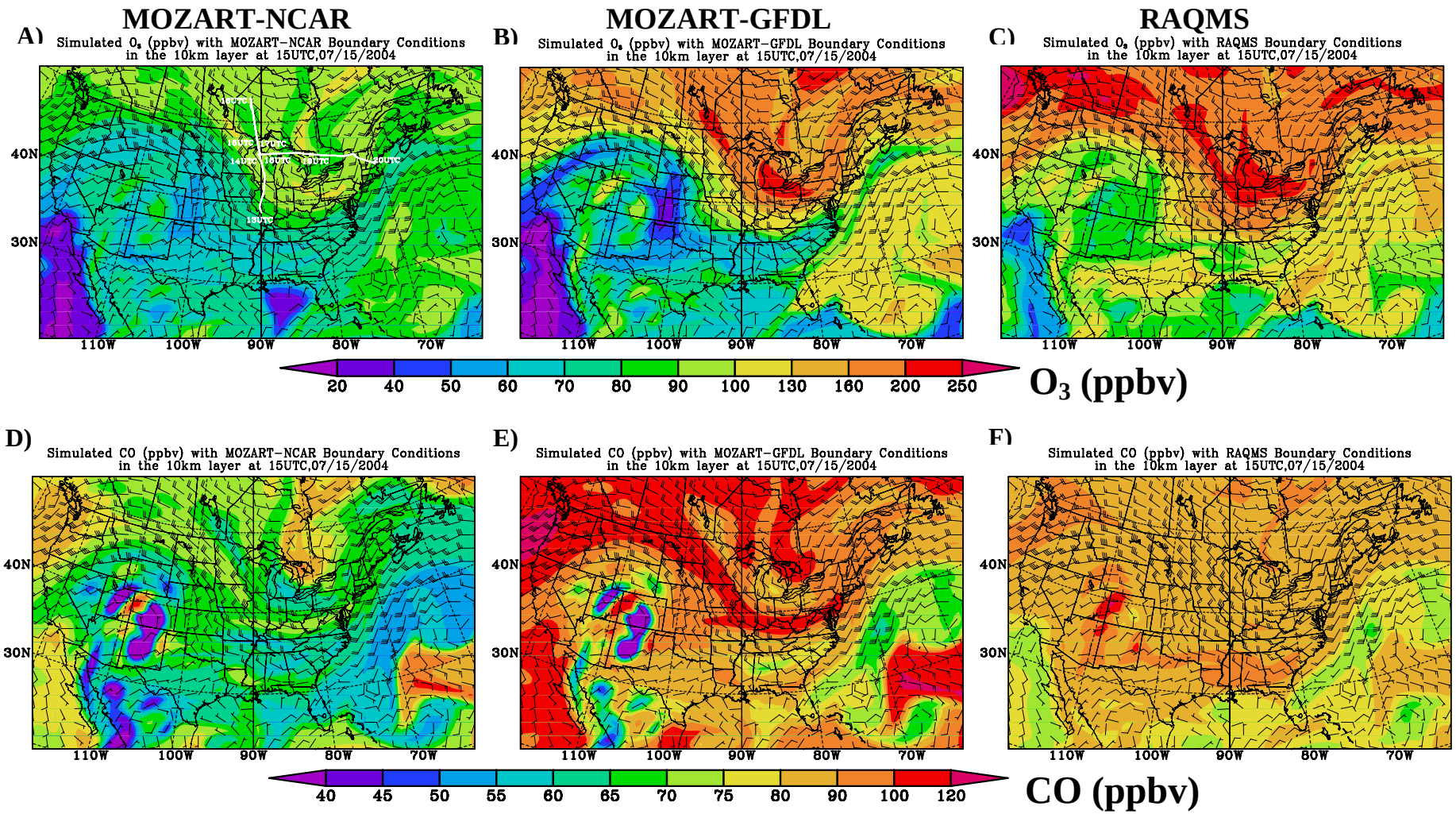

Figure 5. STEM 60km simulated O_3 and CO concentration in the 10km layer with boundary conditions in the 10km layer from the three global models for DC-8 flight 8 on July 15 (plot A shows the flight path).

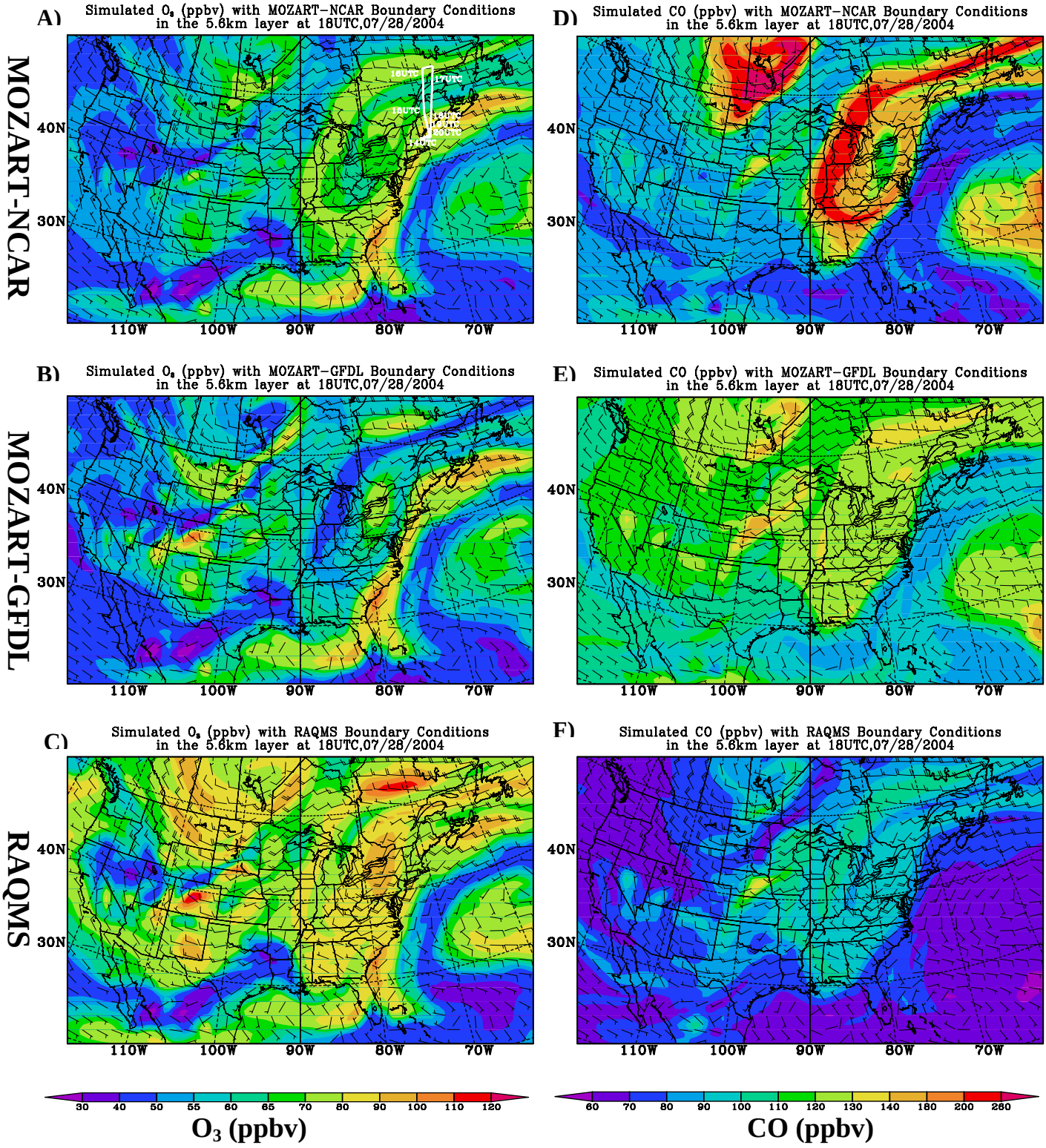

Figure 6. STEM 60km simulated O_3 and CO concentrations in the 5.6km layer with boundary conditions from the three global models for WP-3 flight 12 on July 28 (plot A shows the flight path).

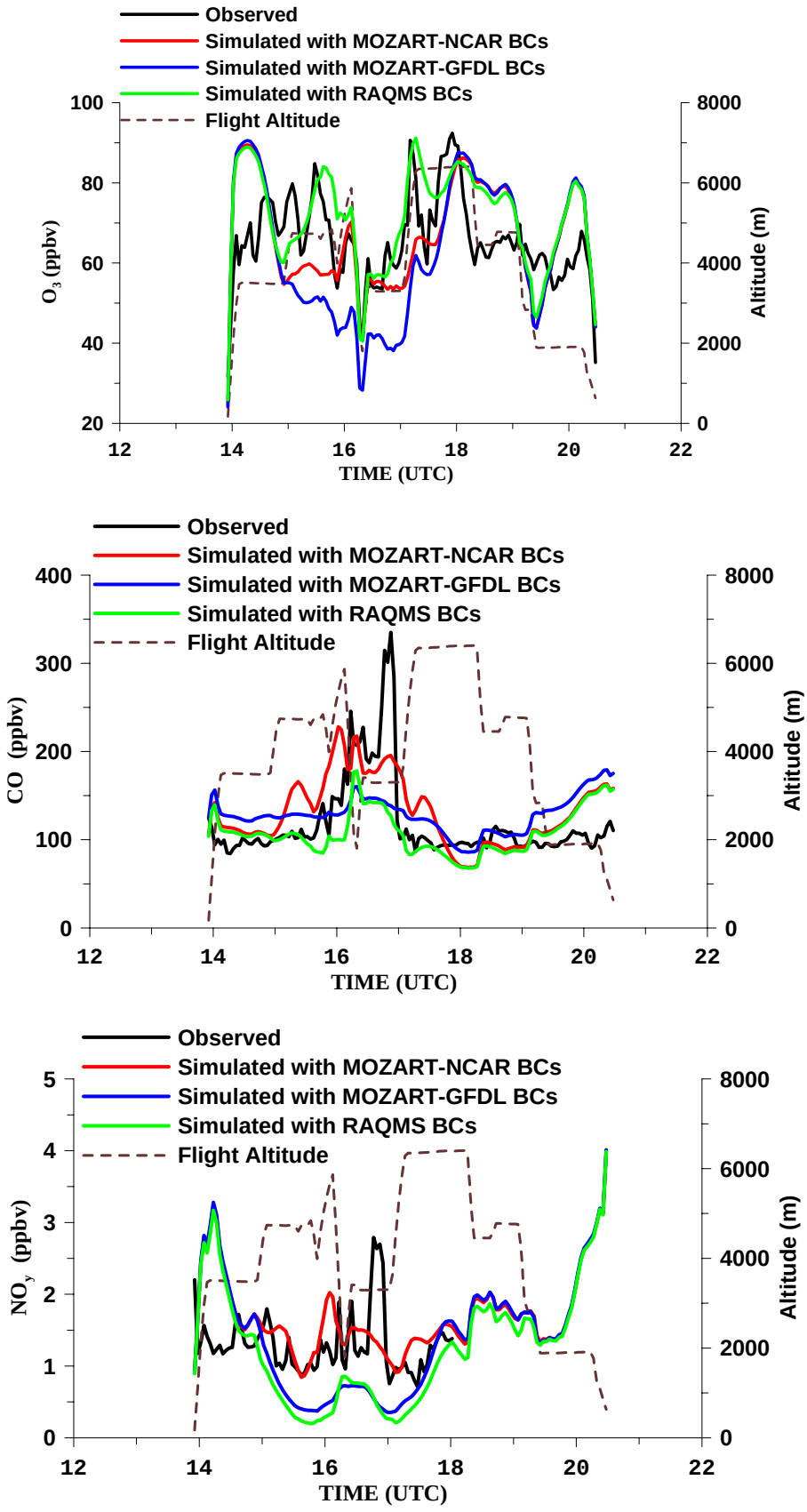

Figure 7. Observed and simulated O_3, CO, and NO_y concentrations for the WP-3 flight 12 on 07/28/2004

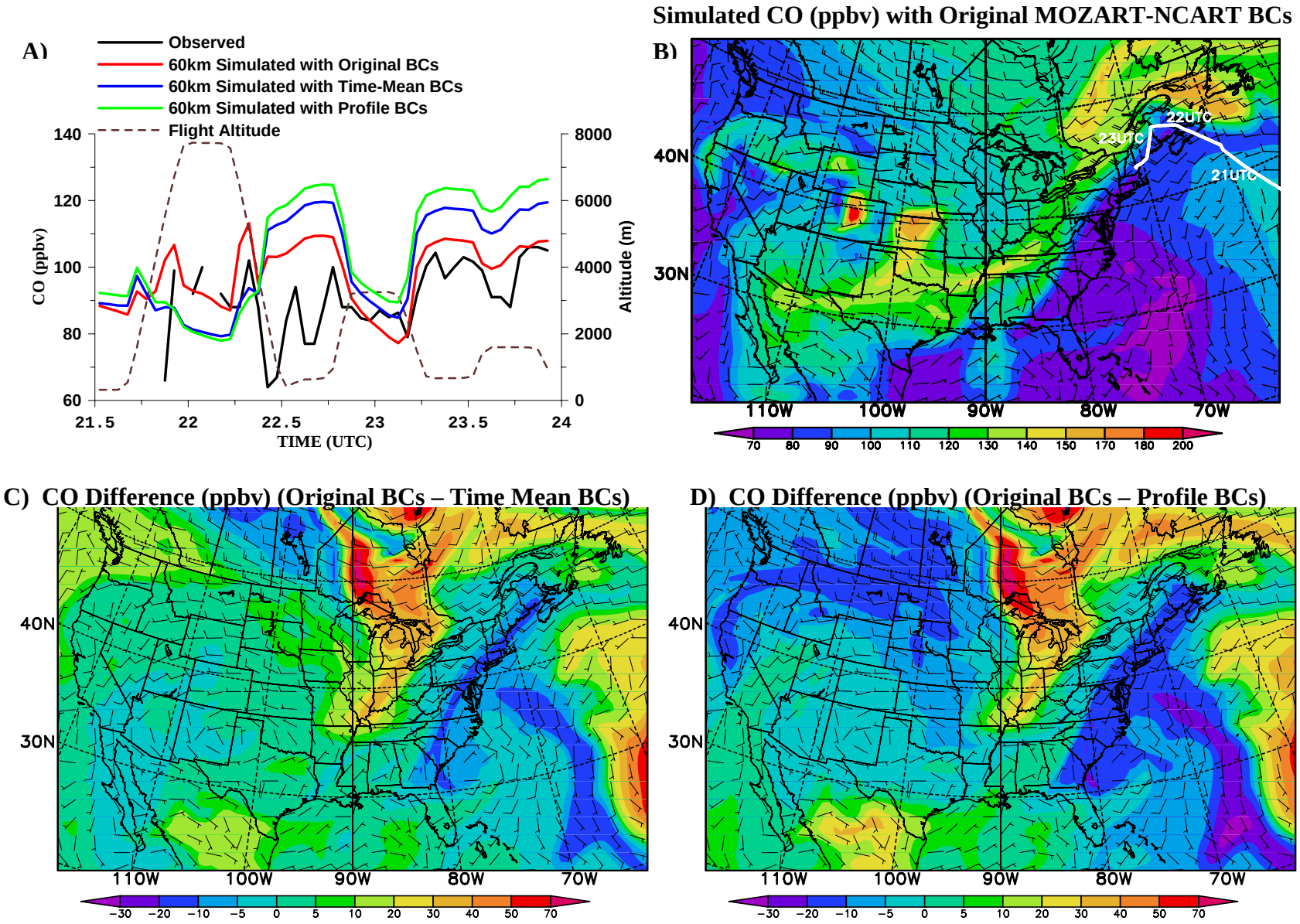

Figure 8. 60km simulated CO compared to the DC-8 flight observation on 07/31/2004. Plot B shows the simulated CO with original MOZART-NCAR BCs in the 3km layer, 0UTC, 08/01/2004. Plots C, D show the corresponding CO differences among the three simulations.

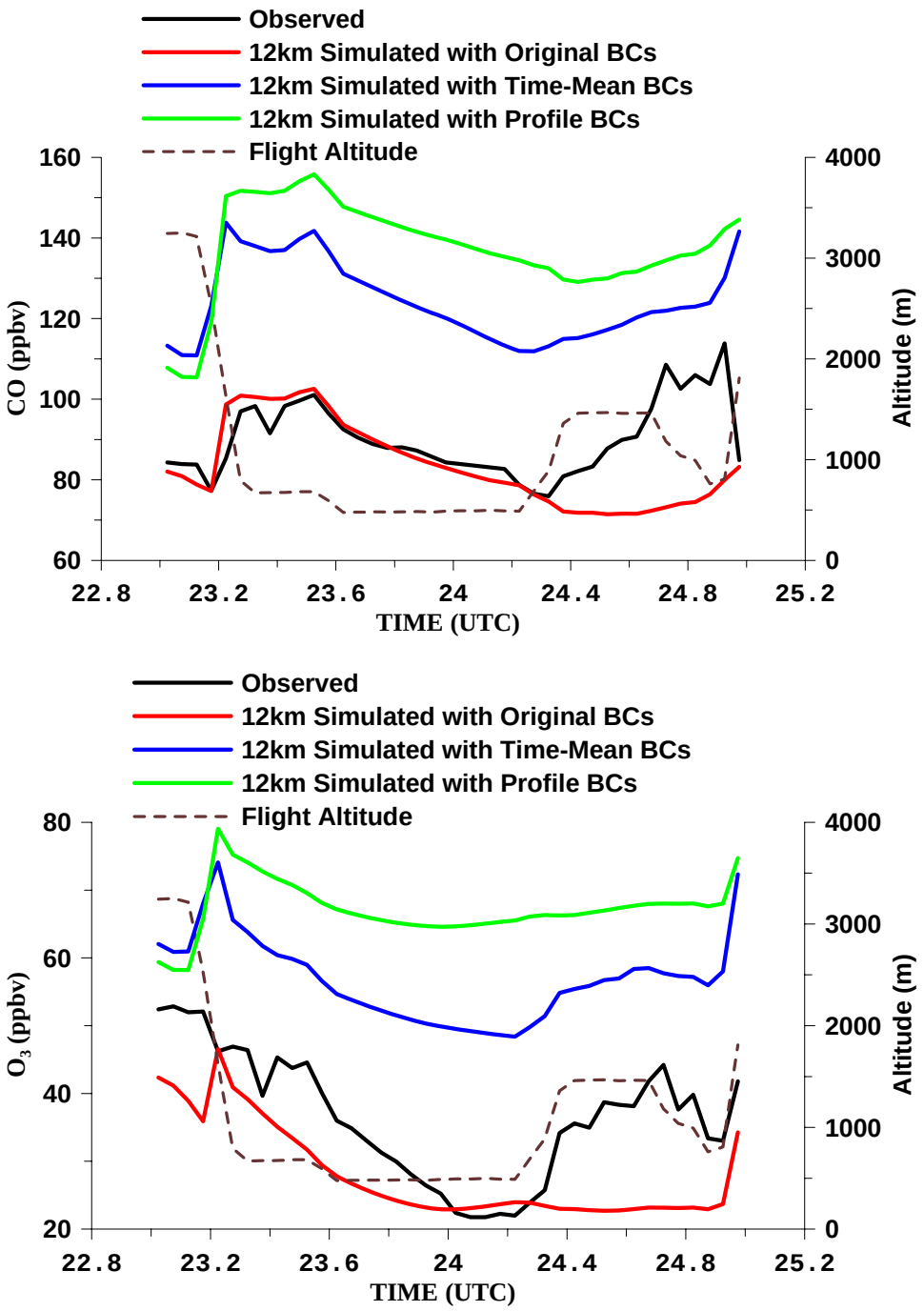

Figure 9. Observed and simulated CO and O_3 concentrations for the WP-3 flight 13 on 07/31- 08/01, 2004

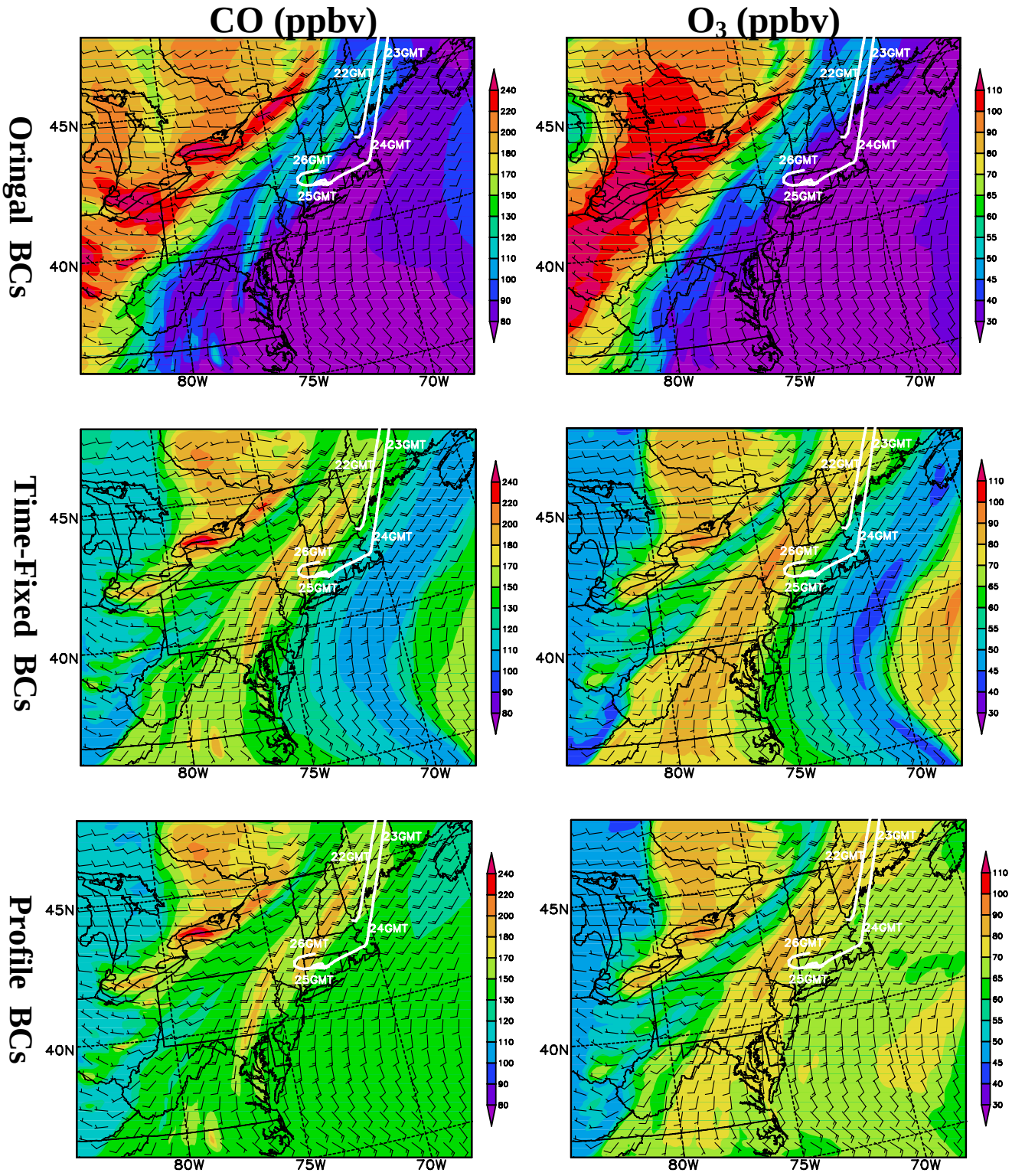

Figure 10. 12km simulated CO (left column) and O_3 (right column) concentrations in the 1km layer, at 0 UTC, 08/01/2004, driven by 3 different boundary conditions. The WP-3 flight path is shown in each plot.

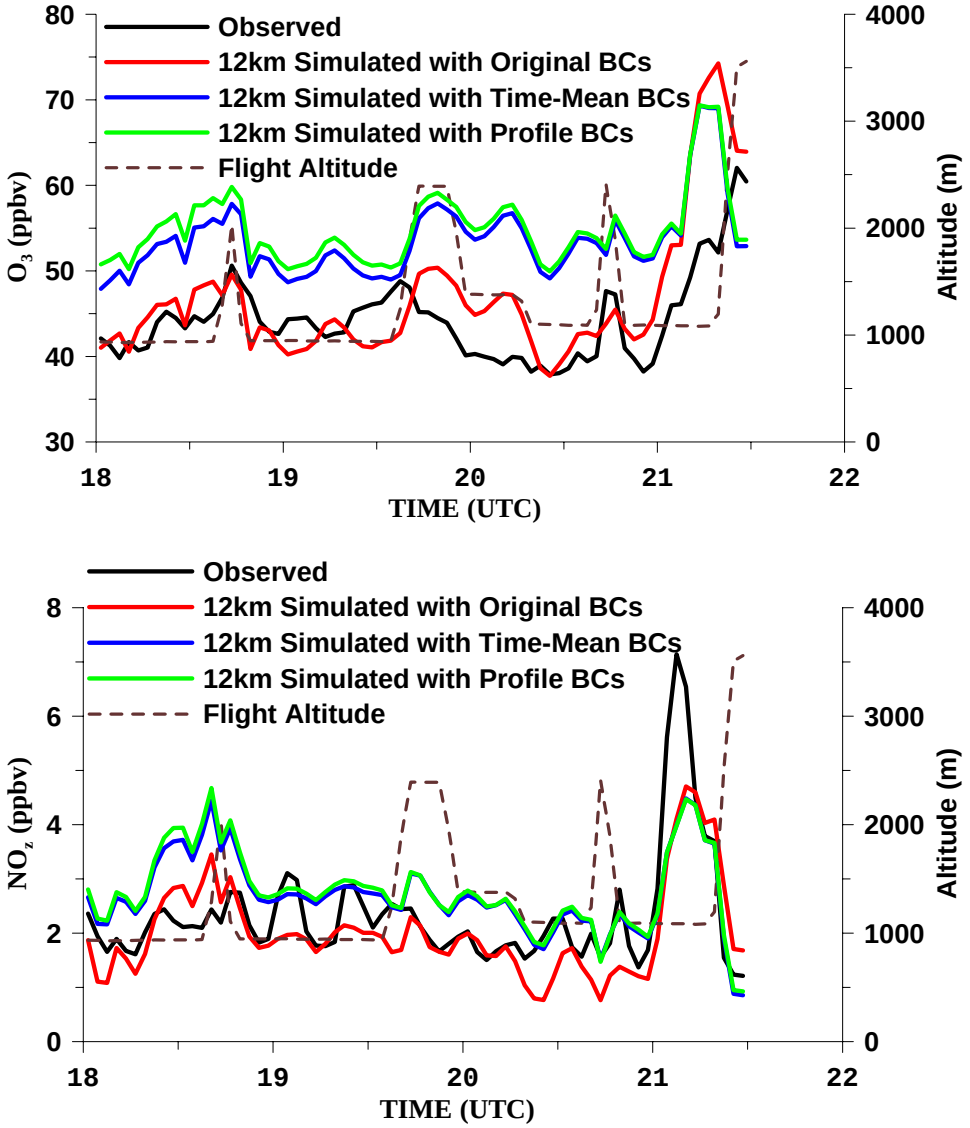

Figure 11. Observed and simulated O_3 and NO_z concentrations for the WP-3 flight 15 on 08/06/2004

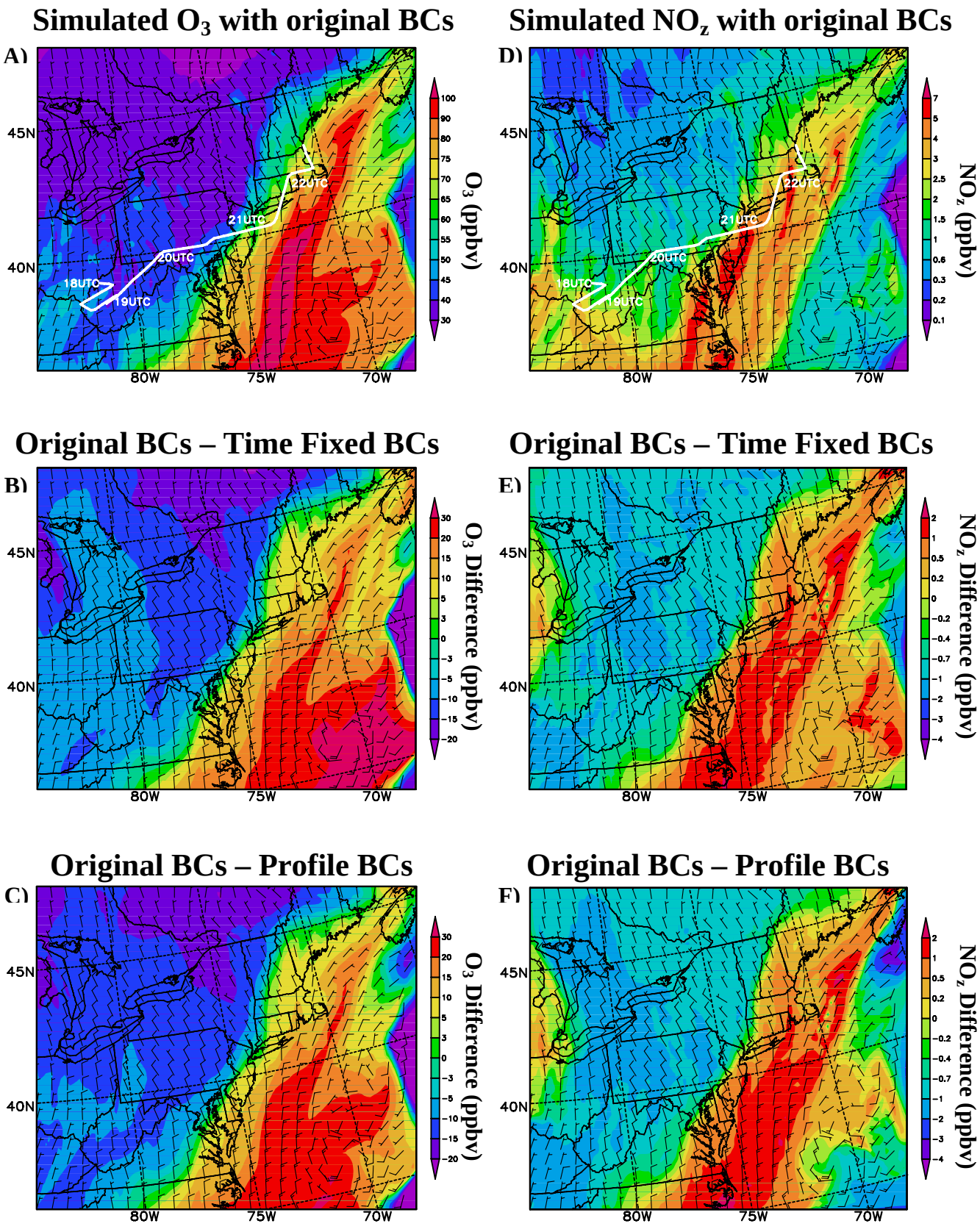

Figure 12. The 12km simulated O_3 and NO_z concentrations and their differences among the three simulations in the 1km layer, 18UTC, 08/06/2004.

NASA DC-8 Flight Paths during ICARTT Period

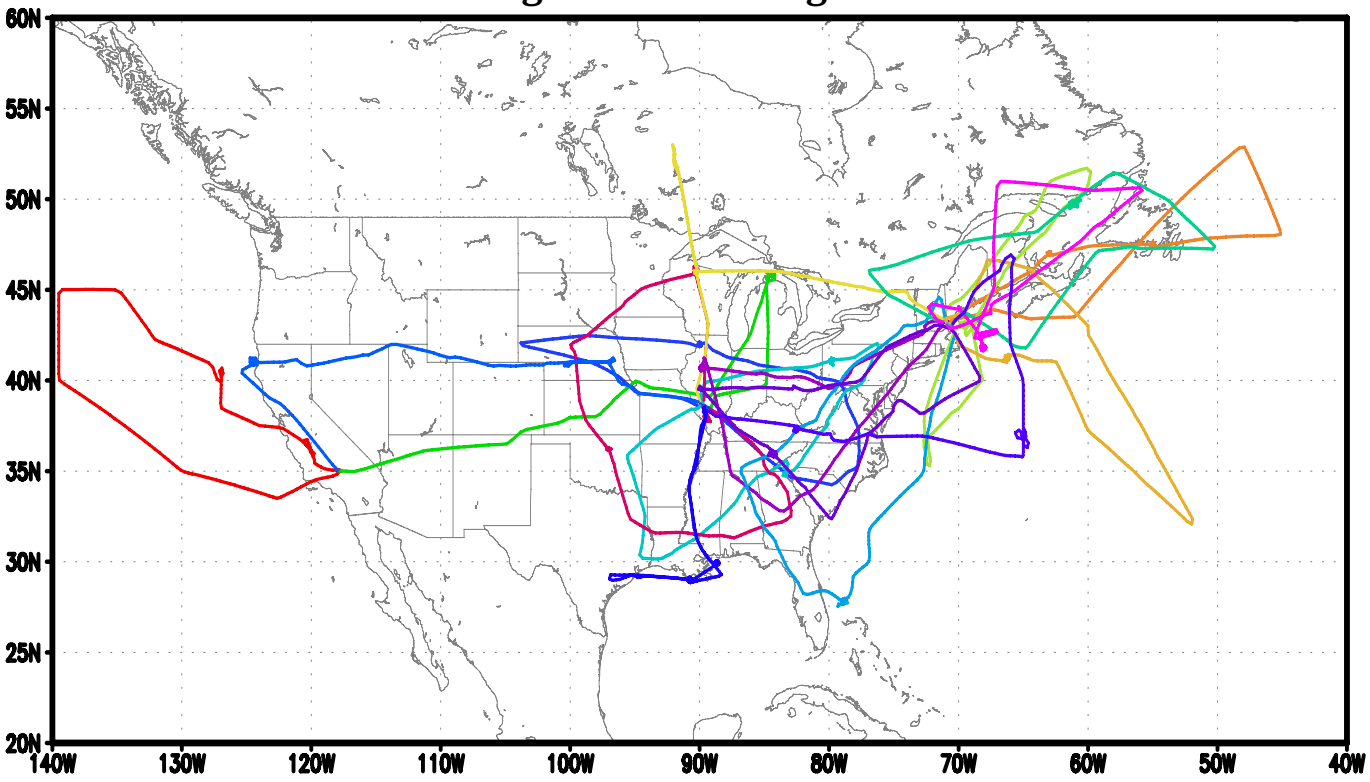

NOAA WP-3 Flight Paths during ICARTT Period

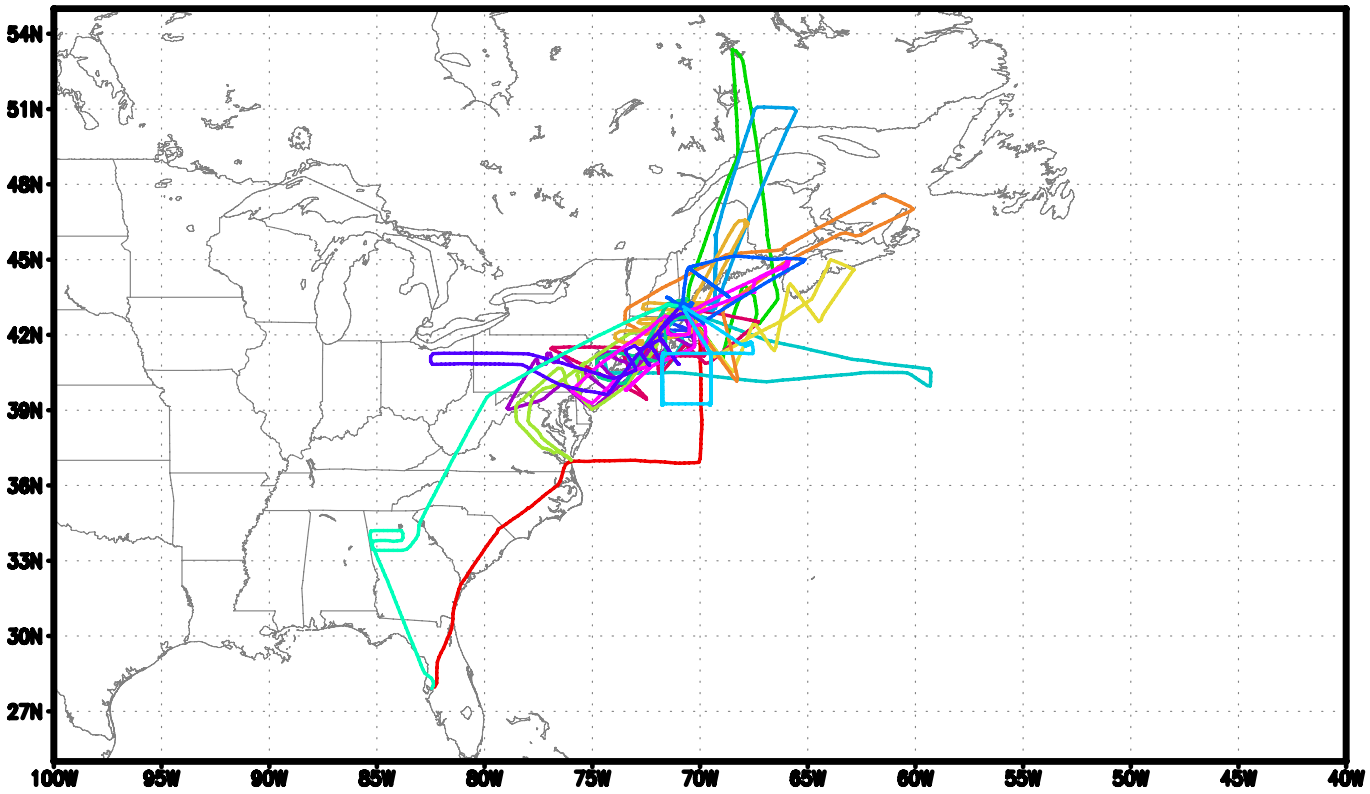

Figure 13. DC-8 and WP-3 flight paths during the ICARTT period

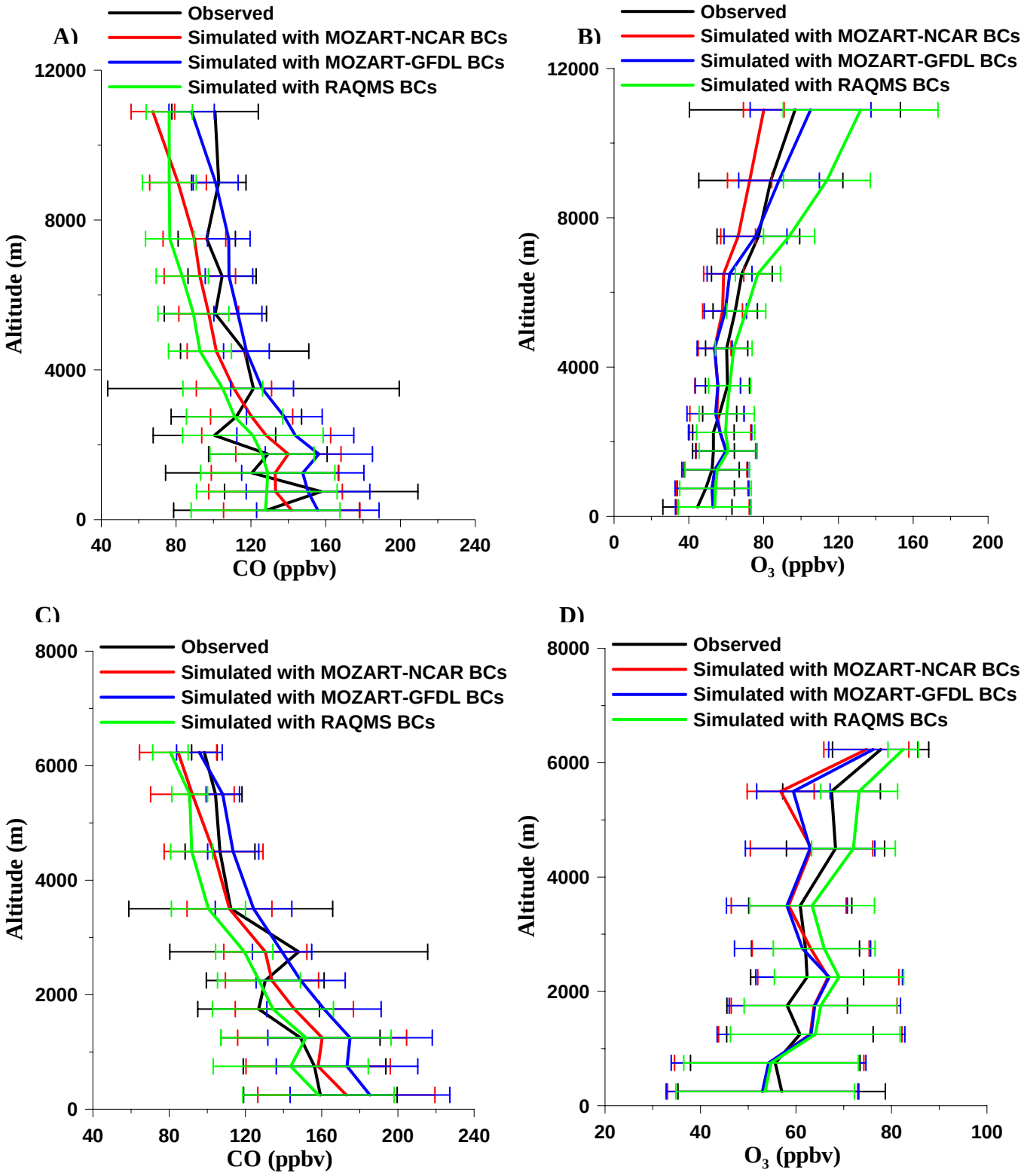

Figure 14. Observed and 60km-simulated CO and O_3 mean profiles and standard deviations for all DC-8 flights (A, B) and WP-3 flights (C, D)

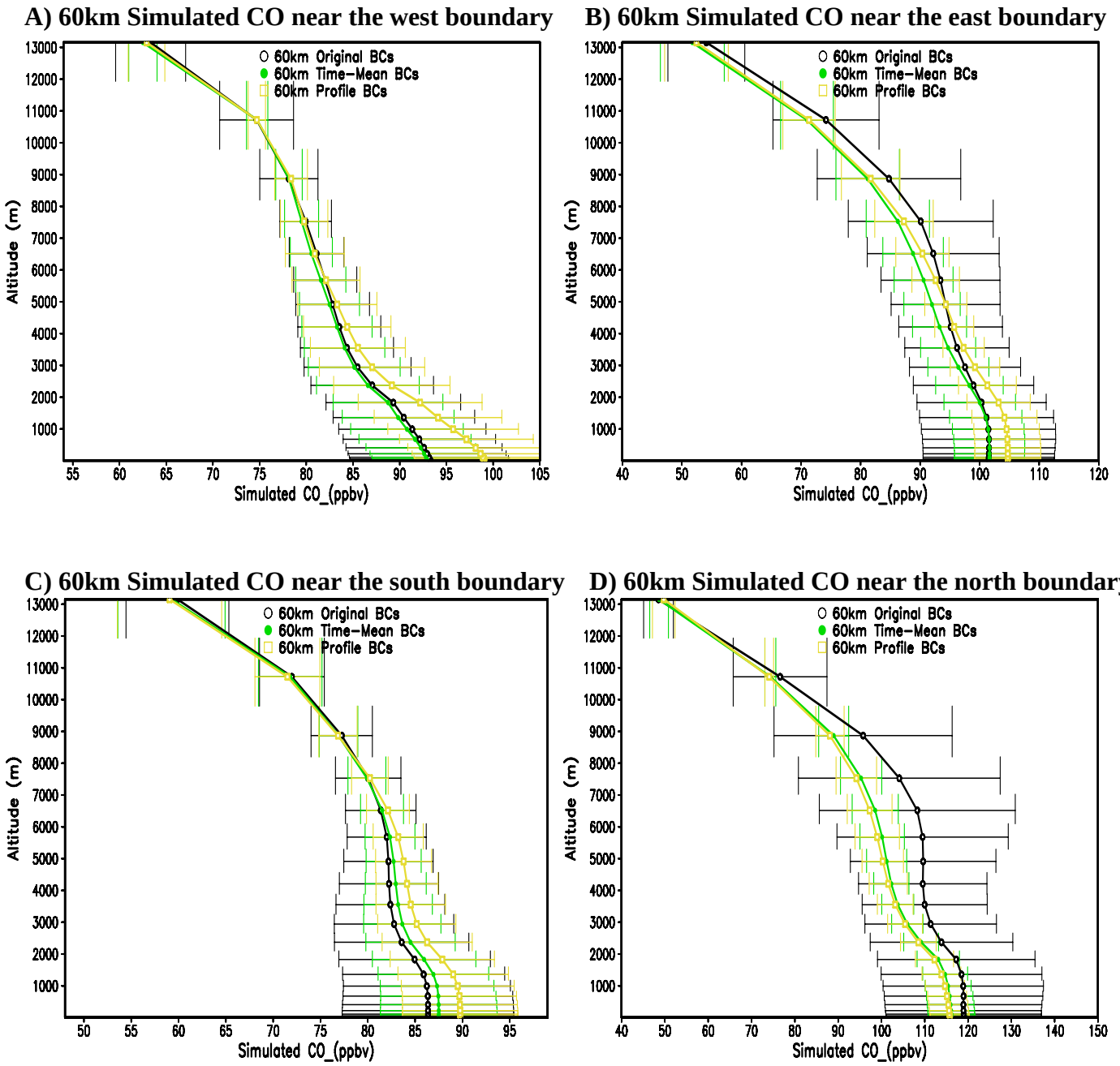

Figure 15. Simulated CO mean concentrations and standard deviation with original MOZART-NCAR, time-mean and profile boundary conditions over the grid lines that are 5 grid cells from west (A), east (B), south (C) and north (D) boundaries, respectively in the 60km domain.

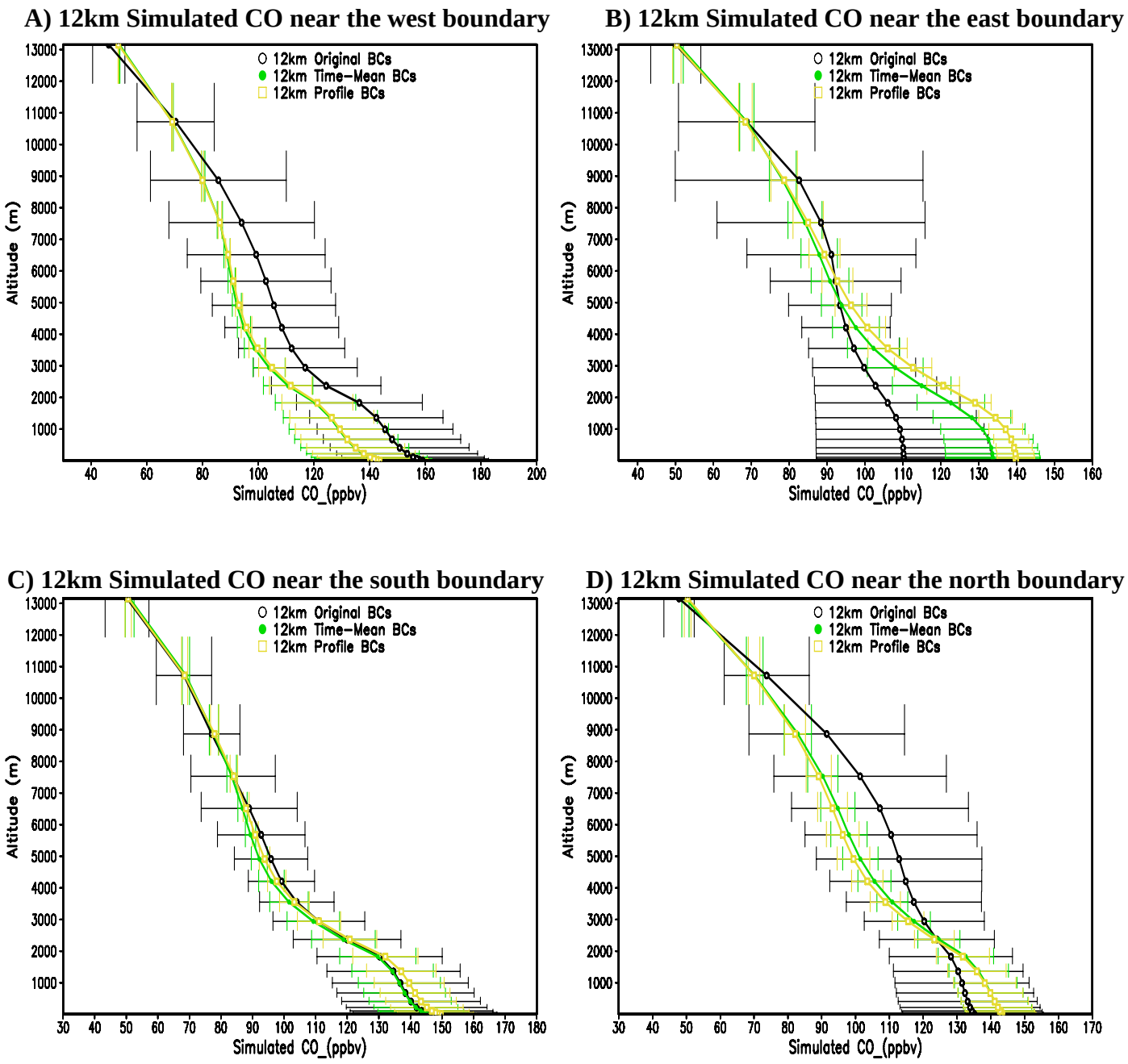

Figure 16. Simulated CO mean concentrations and standard deviation with original time-varied, time-mean and profile boundary conditions over the grid lines that are 5 grid cells from west (A), east (B), south (C) and north (D) boundaries, respectively in the 12km domain.